Int. J. Heat Mass Transfer. Vol. 29, No. 4, pp. 517–527, 1986
Printed in Great Britain

0017–9310/86 $3.00+0.00
Pergamon Press Ltd.

Thermohydrodynamics of quasi-stable floating of a free liquid volume over a solid surface

S. S. KUTATELADZE

Institute of Thermophysics of the Siberian Branch of the U.S.S.R. Academy of Sciences, Novosibirsk, U.S.S.R.

(*Received* 17 *July* 1985)

Abstract—Consideration is given to the main trends in heat and mass transfer during free, stabilized (in the statistical sense) floating of liquid spheroids over a heated surface or over a microporous surface through which a cold gas is injected. Based on the analysis of the experimental data available in the literature, the main mechanism operative in holding up a floating spheroid during intensive heat transfer (or intensive injection) is shown to be the resistance to the vapour (gas) outflow from the periphery of the gap between the bottom of the spheroid and the underlying surface.

THE HISTORY of research into the floating of liquid drops over a hot surface begins with a paper by Leidenfrost (1756), though the dances of water and milk drops on a hot kitchen stove have been observed by housewives from time immemorial. This phenomenon served in the first half of the 19th century as one of the last 'proofs' for the existence of a thermogen. It was also assumed to be one of the specific states of substance, and Boutigny (1840) suggested the term "the spheroidal state of liquid" due to the "repulsive thermal force". The correct idea that such floating is maintained by evaporation was advanced by several researchers in the last century (Bandrimont, 1836; Person, 1842; Armstrong, 1845). Berger (1863) described the oscillations of the form of floating drops. The detailed review of the state of this problem by the last quarter of the 19th century and the accurate experimental confirmation of the existence of a gap between a floating drop and a heated surface are due to Gesekhus [1].

In our time this phenomenon is of interest both as an analogue of some complex regularities of the thermohydrodynamics of boiling and as a method to transfer heat and mass in many technological processes connected with the evaporation of liquids and condensation of vapour.

The floating of arbitrary freely spreading liquid volumes over a heated surface was described by the present author and Borishansky [2], the author's first post-war co-worker. Subsequently, the latter devoted his candidate thesis to this problem [3]. It was at this time that an analogy was shown to exist between the heat transfer to a free liquid volume evaporating on a heated surface and heat transfer from a heated surface placed into a large volume of boiling liquid (Figs. 1 and 2).

To describe the process of floating, the present author suggested a hydrodynamic model which he had begun to develop for the critical phenomena in boiling [2, 4, 5].

Later Baumeister considered a somewhat different hydrodynamic model and, together with Hamill and Schoessow, offered a generalized correlation for a number of experimental data [6].

Recently Goldshtik, Khanin and Ligai, the Institute co-workers of this author, have performed direct experiments to verify the analogy between 'hot' and 'cold' floating of free liquid volumes over an underlying solid surface [7]. They used a microporous plate in much the same way as had been done in the experiments of Malenkov and this author on the displacement effect in a large volume of freely circulating liquid [8]. All of the main shapes of liquid drops floating over a heated surface have been reproduced: quasi-spherical drops, flat and bubbly spheroids. Interesting experiments on the behaviour of a free liquid surface in the vicinity of a heated rod have been carried out by the author's co-workers Avksentyuk and Bochkarev [9].

Furthermore, some other experimental results have been published, e.g. in refs. [10, 12]. All these have prompted this author to return to the problem of the floating of liquid drops.

This paper offers a certain hydrodynamic generalization for the basic characteristics of evaporation of liquid volumes freely floating over a solid base. Thus, a stabilized floating is considered to which there corresponds the right branch of the function $t(\Delta T)$ after the passage through the maximum.

The quasi-static deformation of a freely floating liquid volume, i.e. a change in the relation between its averaged linear characteristics, is determined by the interaction of capillary and gravitational forces. Taking the quantity $\delta_{g\sigma} = (\sigma/g\Delta\rho)^{1/2}$ as the linear scale of this interaction, the following dimensionless quantities can be introduced

$$\bar{V}_{g\sigma} = V/\delta_{g\sigma}^3, \quad \bar{R}_{g\sigma} = R/\delta_{g\sigma}. \tag{1}$$

At $\bar{R}_{g\sigma} \ll 1$, a drop has a shape close to spherical. At $\bar{R}_{g\sigma} > 1$, a liquid spheroid becomes progressively flatter. In the limit, the thickness of a freely spreading liquid becomes of the order of $2\delta_{g\sigma}$. However, this is a great idealization, and a floating spheroid still differs from that located on the underlying non-

NOMENCLATURE

a heat diffusion [$m^2\ s^{-1}$]
c specific heat [$J\ kg^{-1}\ K^{-1}$]
D diameter
D_e equivalent diameter, $(6V/\pi)^{1/3}$ [m]
D diffusion [$m^2\ s^{-1}$]
F heat transfer surface [m^{-2}]
g free fall acceleration [$m\ s^{-2}$]
q heat flux density [$W\ m^{-2}$]
R radius [m]
r latent heat of evaporation [$J\ kg^{-1}$]
T temperature [K]
ΔT 'solid surface–saturation' temperature difference, $T_w - T_s$ [K]
t time [s]
U velocity of motion [$m\ s^{-1}$]
V volume [m^3].

Greek symbols
α heat release [$W\ m^{-2}\ K^{-1}$]
δ thickness of a spheroid [m]
λ thermal conductivity [$W\ m^{-1}\ K^{-1}$]
μ dynamic viscosity [Pa s]
ν kinematic viscosity [$m^2\ s^{-1}$]
ρ density [$kg\ m^{-3}$]
$\Delta\rho$ $= \rho_l - \rho_v$
$\overline{\Delta\rho}$ $= \rho/\rho_l$
$\bar{\rho}_v$ $= \rho_v/\rho_l$
σ surface tension [$N\ m^{-1}$]
σ_r emissivity [$W\ m^{-2}\ K^{-4}$].

Similarity numbers
Ar_* non-standard form of Archimedes number typical of the phenomenon in question, $g\Delta\rho\delta_{g\sigma}^3/\rho_v a_v^2$
K thermal criterion of phase transitions, $r/c_v\Delta T$
Nu_* Nusselt number based on the scale of capillary gravitational interaction, $\alpha\delta_{g\sigma}/\lambda_v$ [$\delta_{g\sigma} = (\sigma/g\Delta\rho)^{1/2}$]
Fr generalized Froude number, $(\rho_v V_{v0}^2)/(g\Delta\rho V^{1/3})$
$\bar{V}$ ratio of the spheroid volume at the time instant t to its volume at the initial instant $t = 0$, V/V_0
$\bar{V}_{g\sigma}$ relative volume on the scale of capillary, gravitational interaction $V/\delta_{g\sigma}^3$.

Subscripts
l liquid
v vapour, gas
ev evaporation
0 characteristic state at a certain instant of time.

Superscript
$\bar{}$ denotes non-dimensional quantities.

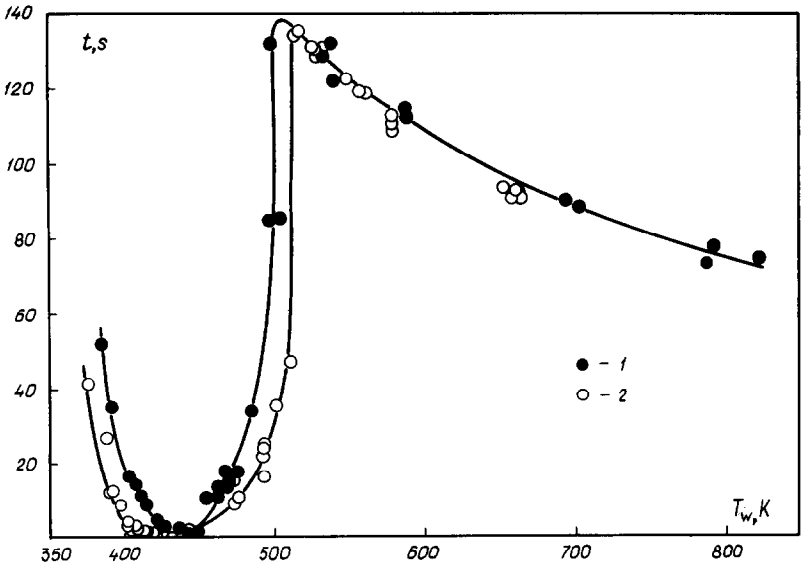

FIG. 1. Vaporization time of a quasi-spherical water drop vs the temperature of a heated surface. The surrounding medium is air at atmospheric pressure. The initial volume of the spheroid is 46–48 mm^3. The heated surface is made of brass 2 mm (1) and 8 mm (2) thick. One can observe the effect of the accumulating capacity of the heated surface at the stages of intensive heat transfer and the independence of stabilized floating of this factor ($\Delta T > 150$ K). The left branch of the curve $t(\Delta T)$ corresponds to nucleate boiling ($\Delta T < 75$ K). The transitional area is in the range $75 < \Delta T < 150$ K.

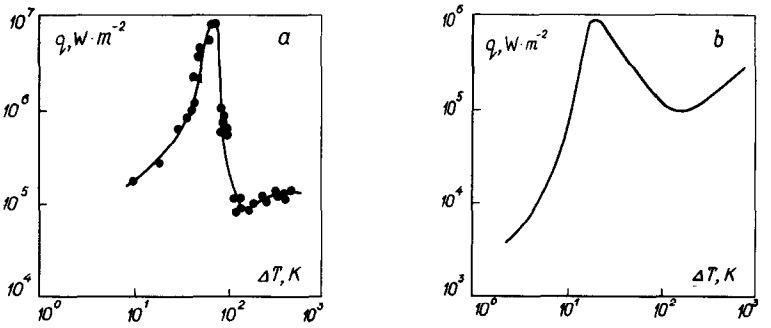

FIG. 2. $\langle q \rangle$ vs ΔT: (a) evaporation of a spheroid; (b) boiling on a heated surface immersed into a large volume of a freely convecting saturated liquid (water at atmospheric pressure).

wettable surface. In the case of a large suspended spheroid there may also occur considerable oscillations in the shape (Fig. 3).

Figure 4 shows the dependence of the diameter and maximum thickness (mean statistical) of spheroids on the equivalent diameter according to the data of refs. [3, 7]. Table 1 lists the thicknesses of bubbly spheroids averaged on the basis of numerous measurements [3].

As is seen, the characteristic thickness of bubbly spheroids is stabilized at the level $\bar{\delta}_1 \approx 3$. The averaged shape of monospheroids (i.e. liquid volumes without inrush of vapour) deviates from both the sphere and disk within the whole interval of their existence. Bubbly spheroids appear at $R \gtrsim 6\delta_{g\sigma}$.

Thus, the absence of strictly canonical shapes of spheroids and their fluctuations makes the theoretical models limited. The last word here belongs to the experiment and similarity analysis within the framework of sufficiently distinct asymptotic models [13].

The mean coefficient of heat transfer to a spheroid, which contains all the mechanisms of heat transfer to the spheroid and its evaporation, for the time t during which the liquid volume changed from V_0 to V, is determined by the elementary heat balance at $r \gg c_l \langle T_l \rangle$:

$$\alpha \Delta T F \, dT = -r\rho_l \, dV; \quad \Delta T = \text{const.}$$

$$\langle \alpha \rangle = \frac{1}{t}\int_0^t \alpha \, dt = \frac{c_v \rho_l K}{t}\int_V^{V_0} \frac{dV}{F}. \tag{2}$$

For a flat spheroid $V = F\delta_l$, $F = \pi R^2$,

$$\langle \alpha \rangle = \frac{c_v \rho_l \delta_l K}{t} \ln \frac{V_0}{V}; \tag{3}$$

for a spherical drop $V = (4\pi/3)R^3$, $F = \Psi \pi R^2$,

$$\langle \alpha \rangle = \left(\frac{48}{\pi}\right)^{1/3} \frac{\rho_l c_v K}{\Psi t}(V_0^{1/3} - V^{1/3}). \tag{4}$$

Here Ψ is the coefficient of the effectiveness of heat transfer of the lower hemisphere. Formula (3) is valid up to the values $R \approx \delta_l$ and formula (4) up to $R = 0$. The latter formula can be used to determine the mean heat transfer rate to quasi-spherical drops from their complete evaporation time t_0 assuming that $\Psi = 1$:

$$\langle \alpha \rangle \approx 2.48 \frac{c_v \rho_l K V^{1/3}}{t_0}. \tag{5}$$

Table 1.

Substance	ρ_l (kg m^{-3})	σ (N m^{-1})	$\delta_{g\sigma}$ (mm)	δ_l (mm)	$\bar{\delta}_l$
H_2O	958	0.059	2.51	7.75	3.09
C_6H_6	817	0.021	1.62	5.20	3.21
CCl_4	1433	0.020	1.20	3.78	3.15
C_2H_5OH	737	0.018	1.52	4.86	3.19

Table 2 presents some experimental results. Here, the value of the vapour gap under a spheroid has been estimated from the experimental value of $\langle \alpha \rangle$ and from the heat conduction mechanism, i.e. it has been assumed that $\langle \delta_v \rangle = \lambda_v / \langle \alpha \rangle$.

There are in fact, five interacting mechanisms for heat transfer of a liquid spheroid with the surrounding medium, i.e. conductive (strictly speaking, conductive–convective) transfer from a heated surface with the

Table 2.

Substance	$c_v \times 10^{-3}$ (J kg^{-1} K^{-1})	$\lambda_v \times 10^2$ (W m^{-1} K^{-1})	$r \times 10^{-5}$ (J kg^{-1})	ρ_l (kg m^{-3})	V_0 (mm^3)	ΔT (K)	K	t_0 (s)	$\langle \alpha \rangle$ (W m^{-2} K^{-1})	$\langle \delta_v \rangle$ (mm)
H_2O	2.137	2.42	22.58	958	46.5	165	6.40	122	958	0.025
						450	2.35	75.0	572	0.012
C_2H_5OH	1.885	1.83	8.25	737	13.6	167	2.62	33.0	653	0.028
						327	1.37	18.8	599	0.030
CCl_4	0.419	0.77	1.88	1433	7.4	305	1.47	11.0	388	0.020

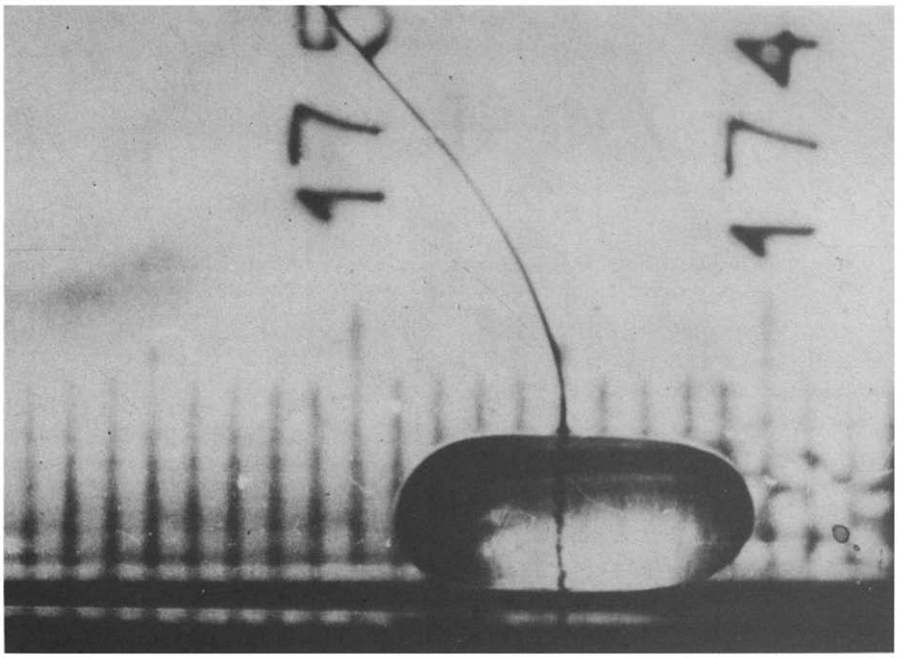

(a)

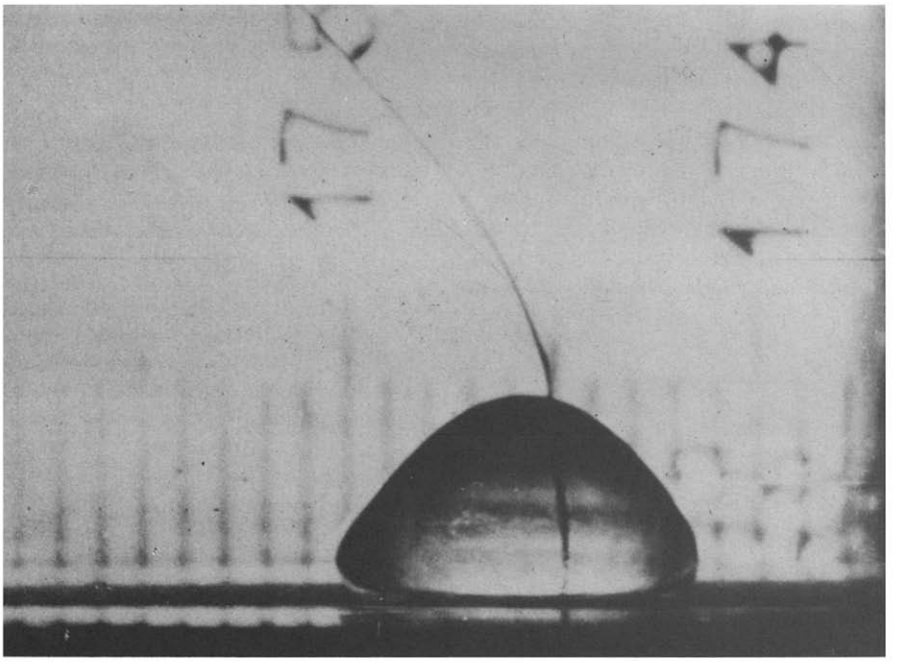

(b)

FIG. 3. Floating of a water spheroid over a microporous surface through which the air is injected. One can observe oscillations of the shape.

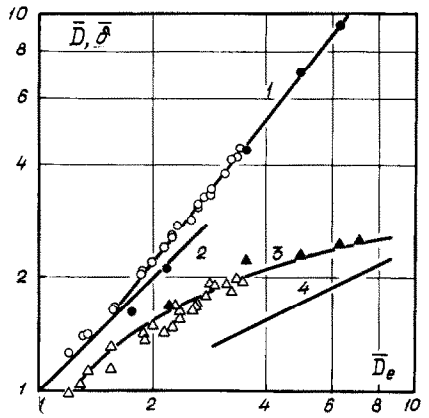

FIG. 4. Dependence of $\bar{D} = D(g\Delta\rho/\sigma)^{1/2}$ (1) and $\bar{\delta} = \delta_l(g\Delta\rho/\sigma)^{1/2}$ (3) on $\bar{D}_e = (6V/\pi)^{1/3}(g\Delta\rho/\sigma)^{1/2}$ on the basis of measurements of spheroids floating over a hot or a cold surface. (2) $\bar{D} = \bar{D}_e$; (4) $\bar{\delta} = (4V/\pi D^2)\,(g\Delta\rho/\sigma)^{1/2}$.

temperature T_w to the lower part of the spheroid where the saturation temperature T_s is attained, corresponding to the pressure $p_0 + g\Delta\rho\delta_l$, where p_0 is the pressure in the surrounding medium; absorption by the spheroid of the incident energy emitted by the heated surface; evaporation from the lower surface of the spheroid to the gap between it and the heated surface; conductive–convective heat transfer from the lower part of the spheroid to its upper part; evaporation from the outer surface of the spheroid into the surroundings.

The radiation heat transfer from the heated surface to the lower part of the spheroid can be estimated as blackbody radiation due to the smallness of the ratio δ_v/R for most of the time that liquid evaporation occurs. In this case the efficiency factor of radiative heat transfer is

$$\alpha_r = \sigma_r(T_w^4 - T_s^4)/\Delta T. \tag{6}$$

For water at $T_s = 373$ K we have the following approximate values of α_r:

T_w (K)	473	573	673	773	873
α_r (W m^{-2} K^{-1})	17.4	25	35	48	64.

The vapour flow in the gap between the lower surface of the spheroid and the heated surface may be assumed to be laminar and, hence, the total coefficient of heat transfer to the spheroid can be determined by the formula

$$\alpha = \lambda_v/\delta_v + \alpha_r. \tag{7}$$

In fact, the Reynolds number of the vapour flow in the gap is of the order

$$Re_v \leqslant U_{vR}\delta_v/\nu_v, \tag{8}$$

where $U_{vR} = U_{v0}R/2\delta_{vR}$ is the vapour outflow velocity around the periphery of the gap, R is the radius of the outflow zone, $U_{v0} = (\alpha\Delta T - q_l)/r\rho_v$ is the outflow velocity per unit surface under the spheroid, δ_{vR} is the gap thickness at the radius R, q_l is the density of the heat flux to the body of the spheroid. The estimates based on the above experimental values of α show that the mode of vapour flow in the gap under the spheroid is in fact laminar.

The mechanism of heat transfer through the spheroid is conductive–convective, since on the surface there exists the temperature gradient $\partial T/\partial x$ and, correspondingly, the surface tension gradient $(\partial\sigma/\partial T)(\partial T/\partial x)$, which causes thermocapillary convection in the spheroid. This gradient has maximum values within the equatorial region of the spheroid and causes eddy flows inside it. Along with this, the friction effect of the vapour outflowing from under the spheroid can be noted.

The minimum heat flux through the spheroid in the quasi-steady approximation is determined by pure heat conduction

$$q_l \approx \frac{\lambda_l}{\delta_l}(T_s - T_l). \tag{9}$$

Here T_l is the mean temperature of the outer surface of the spheroid.

The minimum evaporation rate from the outer surface of the spheroid is determined by the molecular diffusion of vapour into the surrounding medium:

$$q_{ev} = Ar\Delta\rho_v D_v/R. \tag{10}$$

In the case of a quasi-spherical drop, evaporation occurs from the upper hemisphere, i.e. from the surface $\approx 2\pi R^2$ and $A = 1$, and for a flat spheroid—from the outer surface πR^2 and $A = 4/\pi$.

The difference $\Delta\rho_v$ is determined by the density of the saturated vapour at the temperature of the outer surface of the spheroid, T_l, and by the vapour density in the undisturbed region of the surrounding medium.

As is seen from formulae (9) and (10), the evaporation from the outer surface of the spheroid depends only on the physical properties of the liquid and its saturated vapour and also on the diffusion and concentration coefficients of the vapour of the given substance in the surrounding medium. Therefore, the efficient coefficient of heat transfer to the surrounding medium due to evaporation from the spheroid outer surface is

$$\alpha_{ev} \approx AD_v r\Delta\rho_v/(R\Delta T), \tag{11}$$

and decreases with an increasing temperature of the heated surface.

Equating the heat fluxes in formulae (9) and (10), the equation results in determining the temperature on the spheroid outer surface:

$$T_l \approx T_s - D_v r\delta_l\Delta\rho_v/(\lambda_l R). \tag{12}$$

Thus, at $\delta_l \approx R$ the temperature of the spheroid outer surface is virtually independent of its dimensions.

For a water spheroid floating in dry air at atmospheric pressure, the corresponding estimate yields $T_l \approx 350$ K and $\alpha_{ev} = 14(R\Delta T)^{-1}$ W m^{-2} K^{-1}. Hence, for small-size spheroids (i.e. in the final stage of evaporation) and not very high temperatures of the heated surface, the contribution of the external

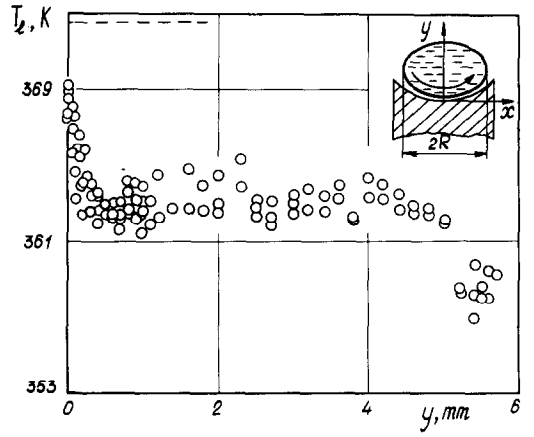

FIG. 5. Temperature profile with respect to the height of a water spheroid, $R = 4.5$ mm, $\Delta T \approx 180$ K. In the top right corner one can see the schematic diagram and the direction of the eddy motion in the spheroid.

evaporation to the heat and mass transfer of a liquid spheroid may be appreciable.

A. A. Bochkarev studied the circulation of liquid in water and ethanol spheroids. He observed the presence in drops of both convection in the form of a single general eddy (water, initial diameter 10 mm) and the generation of paired eddies (ethanol, initial diameter 9 mm and less). As the size of an ethanol drop decreased, the pair of large eddies split and collective motion could be observed. It may well be that the difference between the internal circulation of water and ethanol is due to the capture of surfactants by water. At small diameters (≈ 2 mm) a sharp cessation of liquid circulation was observed.

Figure 5 shows the results of measurements of the temperature profile in a water spheroid floating over a heated surface in the air in normal conditions. One can distinctly see the quasi-isothermal core, i.e. under these conditions the heat transfer from the inner surface to the outer one is practically affected only by eddy thermocapillary convection. Accordingly, the temperature level of the outer surface of the spheroid, T_l, is higher than that in the model of pure heat conduction leading to formula (12). Though the difference in the values of T_l is of the order of several K, however, this leads to an increase in the value of α_{ev} at the expense of an increase of $\Delta\rho_v$ in formula (11).

The basic prerequisite of the hydrodynamic models of the floating of spheroids is reduced to the requirement that the hydrostatic pressure $g\Delta\rho\delta_l$ should be balanced by the corresponding hydrodynamic pressure in the vapour layer on the underlying solid surface. This pressure is created at the cost of the resistance to vapour outflow around the periphery of the spheroid and due to the friction of the vapour flow in the gap.

The first mechanism suggested by this author in 1964 is always necessary, since in its absence there may occur contact of the spheroid periphery with the underlying surface. The second mechanism may affect the formation of bubbly spheroids when the vapour pressure difference between the centre of the gap and its periphery becomes commensurable with the excess hydrostatic pressure. Baumeister ignored these circumstances and adopted the viscous friction in the vapour layer as the basic mechanism.

Consider the relations following from both the models.

The outflow model yields the following relations:

$$\zeta_1^2 g\Delta\rho\delta_l = \rho_v U_{vR}^2/2; \quad U_{vR} = U_{v0}R/2\delta_{vR}, \tag{13}$$

where ζ_1 is the outflow coefficient taking into account also the deformations in the gap and at the outlet cross section. In the case of 'cold' floating

$$\delta_v \approx U_{v0}R\left(\frac{\rho_v}{8\zeta_1^2 g\Delta\rho\delta_l}\right)^{1/2}, \tag{14}$$

in the case of 'hot' floating, when $q_r - q_l \ll \lambda_v\Delta T/\delta_v$,

$$\alpha \approx \frac{\lambda_v}{\delta_v} \approx \left(\frac{\zeta_1\lambda_v(r+\varphi_1 c_v\Delta T)}{\Delta TR}\right)^{1/2}(8g\Delta\rho\rho_v\delta_l)^{1/4}. \tag{15}$$

Here φ_1 is the coefficient of averaging the vapour temperature in the gap, $\varphi_1 \approx 0.5$ (according to the data of ref. [6], $\varphi_1 = 7/20$).

The viscous friction model yields the relations

$$\zeta_2 g\Delta\rho\delta_l \approx \mu_v U_{vR}R/\delta_v^2, \tag{16}$$

for 'cold' floating

$$\delta_v \approx \left(\frac{\mu_v U_{v0}R^2}{2\zeta_2 g\Delta\rho\delta_l}\right)^{1/3} \tag{17}$$

for 'hot' floating, when $q_r - q_l \ll \lambda_v\Delta T/\delta_v$,

$$\alpha \approx \left[\frac{2\zeta_2\lambda_v^3(r+\varphi_1 c_v\Delta T)g\Delta\rho\rho_v\delta_l}{\mu_v\Delta TR^2}\right]^{1/4}. \tag{18}$$

In formulae (14) and (17) U_{v0} is the velocity of gas supply under the spheroid through a microporous surface.

The measure of the relationship between the dynamic pressure (the first model) and the viscous friction (the second model) is the ratio between the RHSs of formulae (14) and (17), i.e. the Reynolds number of the form

$$Re = U_{v0}R/\nu_v, \tag{19}$$

which is independent of the vapour (gas) gap thickness.

The mechanism of molecular friction dominates when $Re < 1$. Using the experimental data of Table 2, one can easily reveal that in the real conditions of the experiments $Re \gg 1$.

Since generally for heat transfer

$$U_{v0} = [\lambda_v\Delta T/\delta_v + \sigma_r(T_w^4 - T_s^4) - q_l](r\rho_v)^{-1}, \tag{20}$$

then the radiative component and the external evaporation partially compensate each other in the determination of U_{v0}, δ_v and α. The parameter which characterizes the total effect of radiation and external evaporation is

$$\bar{q}_{rl} = \frac{q_r - q_l}{r(g\rho_l\rho_v\delta_l)^{1/2}}. \tag{21}$$

The vapour viscosity connected with the thermal conductivity coefficient through the Prandtl number and heat capacity: $c_v\mu_v = Pr_v\lambda_v$, where $Pr_v \approx 1$. Therefore, accurate to the value Pr_v, formulae (15) and (18) differ only in the function of the phase transition criterion $K = r/c_v\Delta T$, i.e. according to the outflow model

$$\bar{\alpha} = \frac{\alpha}{(g\Delta\rho\rho_v\delta_1)^{1/4}}\left(\frac{R}{c_v\lambda_v}\right)^{1/2} \sim (K+\varphi_1)^{1/2}; \quad (22)$$

according to the viscous friction model

$$\bar{\alpha} \sim (K+\varphi_1)^{1/4}. \quad (23)$$

It is these relations which make it possible to ascertain the correspondence of the model to the real process. For this purpose, it is convenient to pass over to the times of vaporization of spheroids.

The time of evaporation from the volume V_0 to the volume V is determined by equation (2) at $\alpha = \lambda_v/\delta_v + \alpha_r$. The value of q_1 exerts an influence only via the value of δ_v, i.e. usually not strongly due to some mutual compensation of q_r and q_1. Therefore, determine the value of α to the first approximation from equations (15) and (18).

For a quasi-spherical liquid volume $\delta_1 \approx R$ and, according to the outflow model,

$$\bar{t} = \frac{t\lambda_v^{1/2}(g\Delta\rho\rho_v)^{1/4}}{\rho_1 c_v^{1/2}(V_0^{5/12} - V^{5/12})} \sim K(K+\varphi_1)^{-1/2}; \quad (24)$$

according to the viscous friction model,

$$\bar{t} \sim K(K+\varphi_1)^{-1/4}. \quad (25)$$

The quantities c_v, λ_v, ρ_v should be related to the temperature $\langle T_v\rangle = T_s + \varphi_1\Delta T$. Practically, to the extent of the accuracy of the measurements available, all the physical properties may be related to T_s, considerably simplifying all calculations.

At $K > 1.5$, the correction for the heat content of the vapour layer, which is characterized by the quantity φ_1, amounts to less than 0.1 in equation (22) and to less than 0.05 in equation (23). Therefore, it is possible to find the preferable model by plotting experimental times for complete evaporation of drops vs the temperature difference $\Delta T = T_w - T_s$ for a given liquid at the same initial volumes and the same pressure of the surrounding medium. Figure 6 presents such data from several experimental series with quasi-spherical drops. The results [10, 12] for carbon tetrachloride cluster about the logarithmic straight lines with the slope $n = -0.5$. The data [3, 10] on water behave in the same way. The data of ref. [11] show a sharper decline in the high-temperature region, and one may draw a logarithmic straight line through them with $n = -0.75$. Closer to this value are also the data on ethanol given in refs. [3, 11].

For large monospheroids approaching the disk form $\delta_1 \approx$ const. $\sim \delta_{g\sigma}$. In this case

$$t \sim \left(\frac{r}{\lambda_v\Delta T g\overline{\Delta\rho}}\right)^{1/2}\left(\frac{\sigma\rho_1}{\bar{\rho}_v}\right)^{1/4}(V_0^{1/4} - V^{1/4}). \quad (26)$$

With allowance for the numerical coefficients in equation (15), formula (26) will have the form

$$t = \zeta_3\left(\frac{r\rho_1\delta_1}{\lambda_v\Delta T}\right)^{1/2}(g\overline{\Delta\rho\rho_v})^{-1/4}(V_0^{1/4} - V^{1/4}), \quad (27)$$

where $\zeta_3 = 4(8\pi)^{-1/4}\zeta_1^{-1/2}$.

Figure 7 presents, in the coordinates of formula (26), the experimental data of ref. [3] on large monospheroids. It is seen that at $V > 0.1V_0$ the dependence $t \sim (V_0^{1/4} - V^{1/4})$ is quite perfectly valid. There is some spread in the experimental points for ΔT. This scatter increases on passing over to the viscous friction model (i.e. from $t \sim \Delta T^{-1/2}$ to $t \sim \Delta T^{-3/4}$).

According to the data of Fig. 7, the proportionality factor in equation (26) is equal to 5. If we assume that $\delta_1 \approx 2.3\delta_{g\sigma}$ (see Fig. 4), then in formula (27) $\zeta_3 \approx 3.3$ and $\zeta_1 \approx 0.3$.

As the volume varies, $V < 0.1V_0$, the evaporation process integrally approaches the law of evaporation of quasi-spheres.

To correlate the experimental data on the times of evaporation of monospheroids, formula (24) was used for $V = 0$ and $\varphi_1 = 0$. The results are given in Figs. 8 and 9 in the coordinates

$$t_0;\ X_1 = \left(\frac{r\rho_1}{\lambda_v\Delta T}\right)^{1/2}(g\overline{\Delta\rho\rho_v})^{-1/4}V_0^{5/12}. \quad (28)$$

For $X_1 < 180$ s the experimental data are better

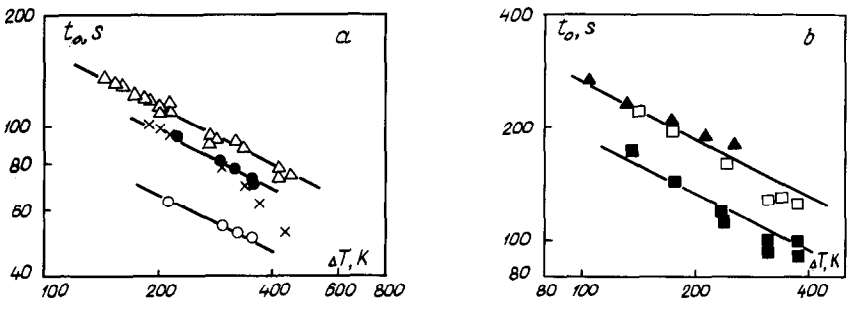

FIG. 6. Total vaporization time of a spheroid vs temperature difference $\Delta T = T_w - T_s$. (a) H_2O: $\triangle$—V_0 = 46 mm³ [3]; ●, ○—V_0 = 30, 15 mm³ [10]; ×—V_0 = 29 mm³ [11]; (b) CCl_4: ▲—V_0 = 8 mm³ [12]; □, ■—V_0 = 8, 4 mm³ [10].

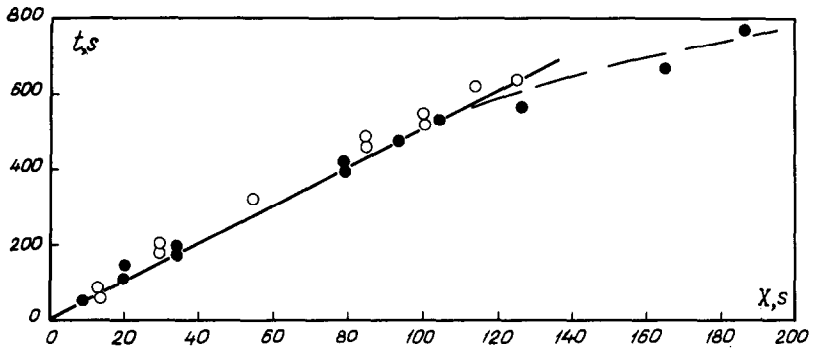

FIG. 7. Vaporization time of large monospheroids vs complex $X = (V_0^{1/4} - V^{1/4})(r/\lambda_v \Delta T g \overline{\Delta\rho})^{1/2}(\sigma\rho_l/\bar{p}_v)^{1/4}$. H_2O: ●—ΔT = 250 K; ○—ΔT = 175 K [3].

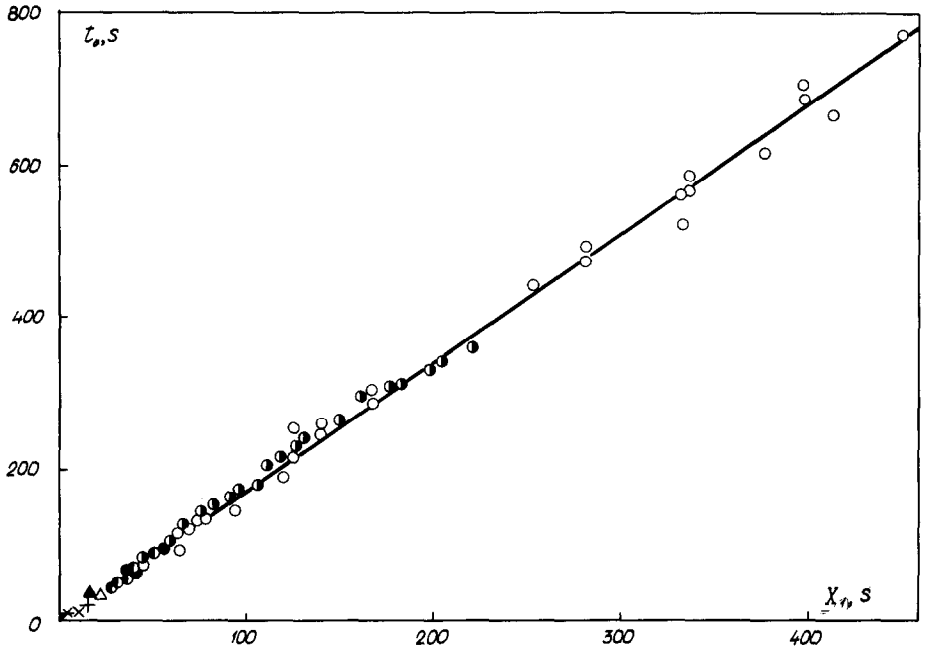

FIG. 8. Total vaporization time of monospheroids vs complex X_1. H_2O: ○—V_0 = 45–5000 mm³ [3]; ●—V_0 = 15–32 mm³ [10]; ◑—V_0 = 15–94 mm³ [12]; ◐—V_0 = 29 mm³; p = 0.13–0.66 MPa [11]. CCl_4: ×—V_0 = 7–9 mm³ [3]; *—V_0 = 4–8 mm³ [10]; +—V_0 = 5–9 mm³ [12]. C_2H_5OH: △—V_0 = 13 mm³ [3]; ▲—V_0 = 6–14 mm³ [10].

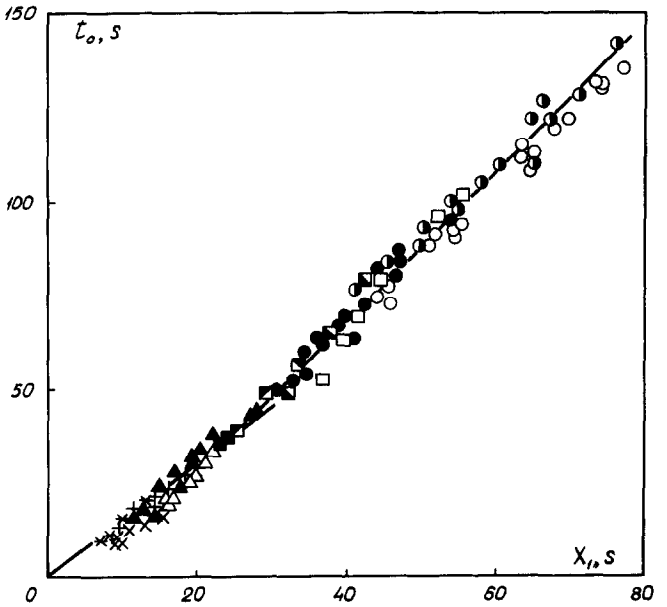

FIG. 9. Data of Fig. 8 on an extended scale at $X_1 < 80$ s. Experiments of ref. [11] at various pressures. (MPa): □—0.13; ◹—0.26; ◹—0.4; ◪—0.53; ■—0.66. The other symbols correspond to those of Fig. 8.

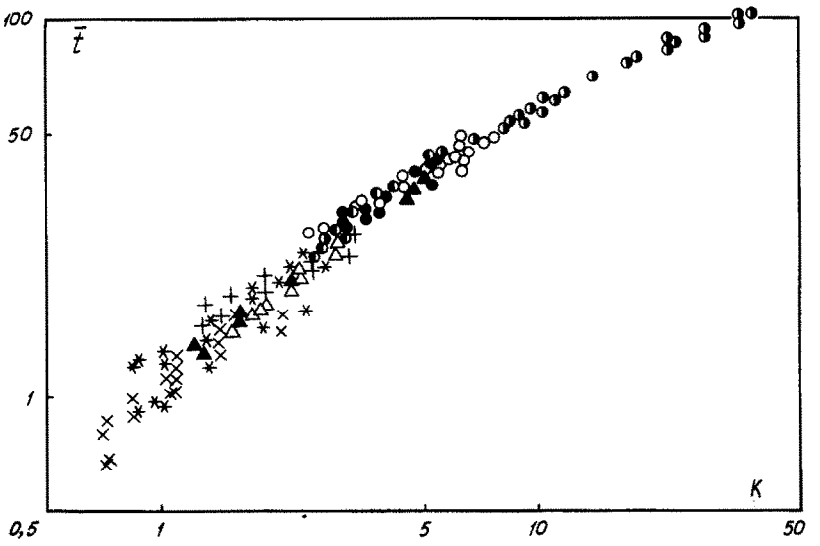

FIG. 10. Data of Fig. 8 in the coordinates $\{\bar{t}, K\}$.

correlated by the relation $t_0 = 1.75X_1$; and for $X_1 > 180$ s by the relation $t = 1.69X_1$. It is virtually possible to assume that $t_0 = 1.7X_1$.

One can assume that the above formulae correctly reflect the most essential trends in the evaporation of spheroids which statistically stably float over a heated surface, since in the experiments analysed, the physical properties, liquid volumes, temperature differences and pressure in the surrounding medium vary within a wide range. This, however, does not exclude the possibility of a certain interaction between the mechanisms of outflow around the spheroid periphery and molecular friction in the inner region of the vapour gap. Therefore, the most suitable semi-empirical correlation of experimental data on monospheroids is their presentation in the coordinates $\{\bar{t}; K\}$. The data of Fig. 8 are presented in these coordinates in Fig. 10.

The heat transfer rate to bubbly spheroids can be estimated with the aid of formula (22) by substituting into it the quantities $\delta_1 \sim R_1 \sim \delta_{g\sigma}$, where R_1 is the effective radius of a liquid volume statistically per one vapour dome. This quantity remains a multiple of the quantity $\delta_{g\sigma}$ until the number of domes attains unity, since in the case of several domes the liquid volume for each of them remains statistically constant.

Then

$$Nu_* \sim Ar_*^{1/4} K^{1/2}. \tag{29}$$

Figure 11 presents the data of ref. [3] in the coordinates of this formula. Here the heat transfer coefficient is related to the total area of bubbly spheroid projection on a heated surface, i.e. also including the area occupied by vapour domes which grow in liquid. The proportionality factor in equation (29), according to these data, is equal to 0.32. It should be noted that the quantity $Ar_*^{1/4}$ has similar values for a number of substances.

The evaporation time of a bubbly spheroid ($V \gtrsim \delta_{g\sigma}^3$), before the appearance of a monospheroid ($V \gtrsim \delta_{g\sigma}^3$) is determined by the conditions $\alpha \approx$ const. and

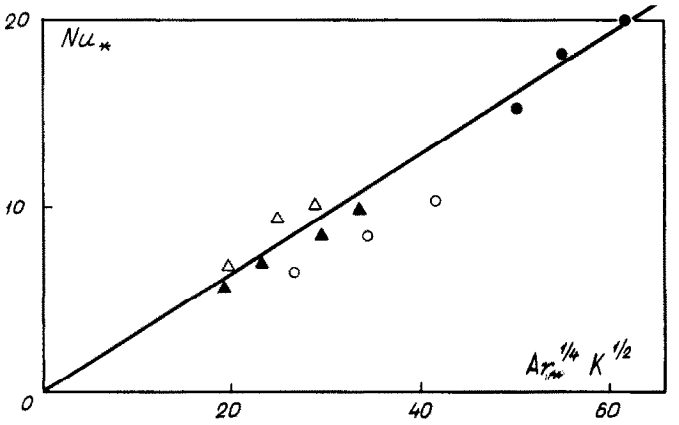

FIG. 11. Dependence of Nu_* on $Ar_*^{1/4}K^{1/2}$ according to the data of ref. [3] for bubbly spheroids: ●—H_2O; ○—C_2H_5OH; △—CCl_4; ▲—C_6H_6.

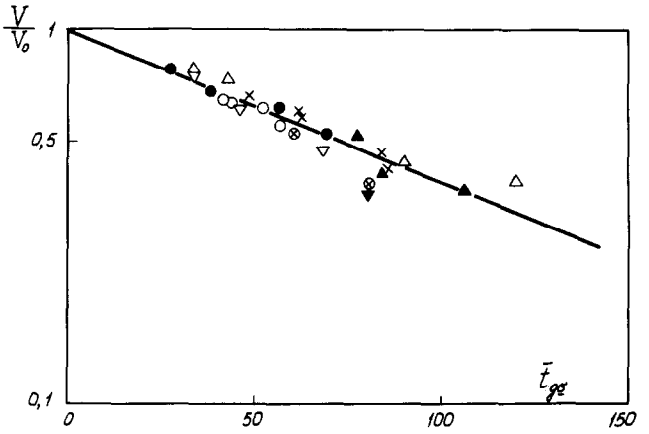

FIG. 12. Relative variation of the volume of a bubbly spheroid in time according to the data of ref. [3]. H_2O: ●—$\Delta T = 250$ K, ○—$\Delta T = 400$ K; C_2H_5OH: △—$\Delta T = 267$ K, ▽—$\Delta T = 407$ K; CCl_4: ▼—$\Delta T = 242$ K, ▲—$\Delta T = 512$ K; C_6H_6: ×—$\Delta T = 260$ K, ⊗—$\Delta T = 450$ K.

$\delta_1 \approx$ const. In this case

$$\bar{t}_{g\sigma} \sim \ln(V_0/V),$$

$$\bar{t}_{g\sigma} = t\left(\frac{\lambda_v \Delta T}{\rho_1 r}\right)^{1/2} \overline{(g\Delta\rho\rho_v)}^{1/4} \delta_{g\sigma}^{-5/4}. \quad (30)$$

Figure 12 gives the corresponding processing of the experimental data of ref. [3].

The floating of a liquid spheroid over a cold permeable surface is not a rigorous analogue of the floating of an evaporating liquid over a hot surface. In the former case, if the experiment is conducted in the same way as in ref. [7], gas is injected through regularly and rather closely spaced small orifices not only beneath the spheroid, but also exterior to it. Thus the outflow from under the spheroid passes over into a forced, upward gas flow around the periphery. Besides, the intensity of gas supply under the spheroid is smaller than that beyond it due to the hydrostatic pressure created by the spheroid. Therefore, the floating of liquid spheroids over a microporous surface depends not only on the Froude and Archimedes numbers and the relative volume

$$Fr = \frac{\rho_v U_{v0}^2}{g\Delta\rho V^{1/3}}; \quad Ar = \frac{g\Delta\rho V}{v_v^2 \rho_v};$$
$$\bar{V}_{g\sigma} = V\left(\frac{g\Delta\rho}{\sigma}\right)^{3/2}, \quad (31)$$

but also on the relationship

$$\overline{\Delta p} = \frac{\Delta p}{g\Delta\rho V^{1/3}}, \quad (32)$$

where Δp is the pressure difference in the permeable plate over which the spheroid is floating. Only at $\Delta p \gg g\Delta\rho V^{1/3}$ the supply of gas to beneath the spheroid will be independent of the size of the latter. The main value sought in this case is the relative thickness of the gap $\delta_v = \delta_v V^{-1/3}$.

Some determination (not very stable) of this quantity has been undertaken in ref. [7]. The thicknesses δ_v are of the same order of magnitude as those in Table 2, but still considerably higher.

Acknowledgements—The author of the paper is grateful to B. P. Avksentyuk, A. A. Bochkarev and M. A. Goldshtik for the discussion of the material of this paper and for the help in preparing some data.

REFERENCES

1. N. A. Gezekhus, The application of electric current to the investigation into the spheroid state of a liquid, *Zh. russk. fiz.-khim. Obschch., Fiz.* **8,** 310, 356 (1876).
2. V. M. Borishansky and S. S. Kutateladze, Some data concerning the evaporation of a liquid in the spheroidal state, *Zh. tekh. Fiz.* **17,** 891–902 (1947).
3. V. M. Borishansky, Heat transfer in a liquid freely flowing over a surface heated to a temperature above the boiling point. In *Problems of Heat Transfer in Change of State* (collected papers, Edited by S. S. Kutateladze), pp. 118–155. Gosenergoizdat, Moscow (1953); Rep. No. AEC-tr-3405, pp. 109–144 (1953).
4. S. S. Kutateladze, Concerning film boiling under free circulation conditions, *Kotloturbostroyeniye* No. 3, 10–12 (1948).
5. S. S. Kutateladze, *Heat Transfer in Condensation and Boiling.* Mashgiz, Moscow (1949, 2nd edn. 1952), Rep. No. AEC-tr-3770 (1959).
6. K. J. Baumeister, T. D. Hamill and G. I. Schoessow, A generalized correlation of vaporization times of drops in film boiling on a flat plate, *Proc. 3rd Int. Transfer Conference*, AIChE, Vol. 4, pp. 66–73 (1966).
7. M. A. Goldshtik, V. G. Ligai and V. M. Khanin, A hydrodynamic analogue of the Leidenfrost phenomenon, Preprint ITF 120-85 (1985).
8. S. S. Kutateladze and I. G. Malenkov, The hydrodynamic analogy between heat transfer and bubble flow crisis in boiling and bubbling. Experimental data, Preprint ITF 100-83, Novosibirsk (1983).
9. B. P. Avksentyuk and A. A. Bochkarev, The interaction of a heated body with a free liquid surface, *Zh. tekh. Fiz.* **55,** 797–798 (1985).
10. B. S. Gottfried, C. J. Lee and K. J. Bell, The Leidenfrost phenomenon : film boiling of liquid droplets on a flat plate, *Int. J. Heat Mass Transfer* **9,** 1167–1187 (1966).
11. G. S. Emmerson, The effect of pressure and surface material on the Leidenfrost point of discrete drops of water, *Int. J. Heat Mass Transfer* **18,** 381–386 (1975).
12. V. Betta, P. Mazzei, V. Naso and R. Vanoli, Further contributions to the study of the Leidenfrost phenomenon, *Trans. Am. Soc. mech. Engrs,* Series C, *J. Heat Transfer* **101,** 612–616 (1979).
13. S. S. Kutateladze, *Similarity Analysis in Thermophysics.* Izd. Nauka, Novosibirsk (1982).

THERMODYNAMIQUE DU FLOTTEMENT QUASI-STABLE D'UN VOLUME LIBRE DE LIQUIDE SUR UNE SURFACE SOLIDE

Résumé—On considère les traits principaux des transferts de chaleur et de masse pendant le flottement de sphéroïdes de liquide stabilisés sur une surface chaude ou sur une surface microporeuse à travers laquelle un gaz froid est injecté. A partir de l'analyse de données expérimentales disponibles dans la bibliographie, le principal mécanisme actif qui maintient un sphéroïde flottant pendant le transfert thermique intensif (ou l'injection intensive) est montré être la résistance à la sortie de vapeur (gaz) de la phériphérie de l'espace étroit entre la base du sphéroïde et la surface sous-jacente.

THERMOHYDRODYNAMIK DER QUASI-STABILEN BEWEGUNG EINES FREIEN FLÜSSIGKEITSVOLUMENS ÜBER EINE FESTE OBERFLÄCHE

Zusammenfassung—Betrachtet wird der Wärme- und Stoffübergang bei der freien, statistisch stabilen Bewegung von Flüssigkeitstropfen über einer beheizten Oberfläche oder über einer mikroporösen Fläche, durch die kaltes Gas eingeleitet wird. Aus experimentellen Daten in der Literatur kann man ersehen, daß der Hauptmechanismus, der einen strömenden Tropfen während des intensiven Wärmeübergangs (oder bei der intensiven Gaseinleitung) stabil erhält, auf dem Widerstand des Dampf- oder Gasaustritts zwischen der Unterseite des Tropfens und der darunterliegenden Fläche beruht.

ТЕРМОГИДРОДИНАМИКА КВАЗИСТАБИЛЬНОГО ВИТАНИЯ СВОБОДНОГО ОБЪЕМА ЖИДКОСТИ НАД ТВЕРДОЙ ПОВЕРХНОСТЬЮ

Аннотация—Рассматриваются основные закономерности тепломассообмена при свободном, стабилизированном витании жидких сфероидов над горячей и микропористой поверхностями, через которые производится вдув холодного газа. На основе анализа имеющихся в литературе экспериментальных данных показано, что при интенсивном теплообмене (или интенсивном вдуве) основным механизмом удержания витающего сфероида является сопротивление истечению пара (газа) с периферии зазора между дном сфероида и подстилающей поверхностью.